

# **Document made available under the Patent Cooperation Treaty (PCT)**

International application number: PCT/US04/041331

International filing date: 09 December 2004 (09.12.2004)

Document type: Certified copy of priority document

Document details: Country/Office: US  
Number: 60/528,081  
Filing date: 09 December 2003 (09.12.2003)

Date of receipt at the International Bureau: 31 January 2005 (31.01.2005)

Remark: Priority document submitted or transmitted to the International Bureau in compliance with Rule 17.1(a) or (b)



World Intellectual Property Organization (WIPO) - Geneva, Switzerland  
Organisation Mondiale de la Propriété Intellectuelle (OMPI) - Genève, Suisse

1274642

# UNITED STATES OF AMERICA

TO ALL TO WHOM THESE PRESENTS SHALL COME:

UNITED STATES DEPARTMENT OF COMMERCE

United States Patent and Trademark Office

*January 19, 2005*

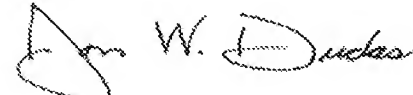
THIS IS TO CERTIFY THAT ANNEXED HERETO IS A TRUE COPY FROM  
THE RECORDS OF THE UNITED STATES PATENT AND TRADEMARK  
OFFICE OF THOSE PAPERS OF THE BELOW IDENTIFIED PATENT  
APPLICATION THAT MET THE REQUIREMENTS TO BE GRANTED A  
FILING DATE.

APPLICATION NUMBER: 60/528,081

FILING DATE: *December 09, 2003*

RELATED PCT APPLICATION NUMBER: PCT/US04/41331

Certified by



Under Secretary of Commerce  
for Intellectual Property  
and Director of the United States  
Patent and Trademark Office





16179 U.S. PTO

Docket: 122302.00009

19587 60/528081 U.S. PTO  
120903

## TRANSMITTAL FORM

Mail Stop Provisional Patent Application  
Commissioner for Patents  
P.O. Box 1450  
Alexandria, VA 22313-1450

CERTIFICATE OF MAILING  
Express Mailing Label Number EV393968185 US  
Date of Deposit December 9, 2003

Dear Sir:

Enclosed application parts are:

Spec w/Claims      Number of Pages 16  
 Spec w/out Claims      Number of Pages \_\_\_\_\_  
 References      Number of Sheets 2  
 Informal Drawings      Number of Sheets 15  
 Small Entity Status Claimed under 37 CFR 1.27

## Inventor(s):

LAST NAME	FIRST NAME	MIDDLE INITIAL	RESIDENCE (CITY, STATE OR FOREIGN COUNTRY)
Hu	Zhibing		Denton, Texas
Xia	Xiaohu		Denton, Texas

TITLE OF INVENTION:  
**HYDROGEL NANOPARTICLE DISPERSIONS WITH INVERSE THERMOREVERSIBLE GELATION**

## CORRESPONDENCE ADDRESS:

Michael G. Cameron.  
Jackson Walker, L.L.P.  
2435 North Central Expressway, Suite 600  
Richardson, TX 75080  
PHONE: (972) 744-2934

Was this invention made under a Government contract?  No  YesIdentify contract and the Government agency: National Science Foundation 0102467

A check is enclosed in the amount of \$80.00. The Commissioner is hereby authorized to charge any additional fees which may be required, or credit any overpayment to Deposit Account No. 50-1752.

Respectfully submitted,



Michael G. Cameron  
Attorney for Applicant(s)  
Reg. No. 50,298

Date: December 9, 2003

**PROVISIONAL APPLICATION ONLY**

**"EXPRESS MAILING"**

Mailing Label No.: EV 393968185 US

Date of Deposit: December 9, 2003

## **HYDROGEL NANOPARTICLE DISPERSIONS WITH INVERSE THERMOREVERSIBLE GELATION**

### Inventors

Zhibing Hu

Xiaohu Xia

### Government Funding

National Science Foundation Award 0102467.

### Summary of the Invention

The present invention comprises (1) The process, technique and apparatus for synthesizing of the mono-disperse nanoparticles with the interpenetrating structure of poly(N-isopropylacrylamide) and poly(acrylic acid), which will be referred as IPN nanoparticles hereafter in this disclosure; (2) Reversible formation of the physically crosslinked nanoparticle networks based on this IPN nanoparticles; (3) Novel drug release carrier on the basis of the physically crosslinked IPN nanoparticle networks.

### Background of the Invention

Hydrogels containing two interpenetrating polymer networks (IPN) have attracted an intensive investigation.<sup>[1]</sup> This is because an IPN hydrogel usually exhibits properties that a hydrogel with the random co-polymerization of two monomers does not have. For

example, the IPN of poly(acrylic acid) (PAAc) and polyacrylamide (PAAM) undergoes the volume phase transition driven by cooperative “zipping” interactions between the molecules which result from hydrogen bonding.<sup>[1]</sup> In addition to the improved mechanical properties which usually come from the reinforcement between two interpenetrating networks,<sup>[2]</sup> an IPN hydrogel can have a preferred direction for swelling by pre-stressing one of them (poly-N-isopropylacrylamide (PNIPAM)) before the gelation of the other one (polyacrylamide (PAAM)) takes place.<sup>[3]</sup> A well-designed hydrogel with an IPN structure shows an upper critical solution temperature without a volume change.<sup>[4]</sup>

Two polymer chain networks in an IPN gel can be sensitive independently to two different external stimuli. Such hydrogels have been employed for controlled drug delivery.<sup>[5-7]</sup> The PNIPAM gel undergoes the volume phase transition at  $T_c=34\text{ }^{\circ}\text{C}$ <sup>[8-13]</sup> and has been used often as one of the components in an IPN gel. Its phase transition temperature remains the same if the PNIPAM is incorporated in an IPN matrix. However, the random copolymerization results in shifting  $T_c$  depending on the hydrophilic/hydrophobicity of the co-monomer.<sup>[7]</sup>

IPN microgel particles have been synthesized because they are more effective as delivery systems than macroscopic gels for agrochemical or medical applications.<sup>[14]</sup> A comparison of the swelling behavior of the random P(AAc-*co*-AAm) particles and PAAc/PAAm IPN microgels has been made using temperature and pH as the triggers.<sup>[14]</sup> Jones and Lyon, on the other hand, showed multiresponsive core-shell microgels that consist of a weakly interpenetrating polymer network core and a shell<sup>[15]</sup>. These microgels were prepared by precipitation polymerization at 70 °C in aqueous media. In

the synthesis of the shell polymer, the collapsed particles serve as nuclei for further polymerization, thereby resulting in preferential growth of the existing particles over the nucleation of new ones.<sup>[15]</sup>

Here we show a method to synthesize an IPN microgel of PNIPAM/PAAc. We extended Jones and Lyon's method<sup>[15]</sup> by controlling reaction time so that the reaction was stopped once the interpenetrating network was formed at room temperature. We present the synthesis and light scattering characterization of these microgels, which displays the same  $T_c$  as the PNIPAM but shrinks less than the PNIPAM above  $T_c$ . The semi-dilute aqueous solutions of the PNIPAM-PAAc IPN microgels exhibit unusually inverse thermo-reversible gelation. In contrast to polymer solutions of poly(NIPAM-*co*-AAc) that have the inverse thermo-reversible gelation,<sup>[16-19]</sup> our system can self-assemble into an ordered structure, displaying bright colors.

#### Brief Description of the Figures

**Scheme 1.** IPN microgel synthesis: (a) a pure PNIPAM miscorgel as a seed; (b) shrunk PNIPAM microgel under the effect of electrolyte acrylic acid, the red dots stand for the acrylic acid monomers; the hydrogen bonding between PNIPAM and acrylic acid was represented by the dot line as indicated in the enlarged chemical structure; (c) polymerization of the acrylic acid; (d) the resultant IPN microgels of PNIPAM-PAAc.

**Figure 1.** Time dependent hydrodynamic radius ( $R_h$ ) of the particles during IPN microgel formation. Here 10 ml of aliquot solution was taken from the reaction container at the different reaction times for dynamic light scattering analysis. All samples have the

same polymer concentration of  $5.0 \times 10^{-6}$  g/ml based on PNIPAM solid content. The pH values were adjusted between 6.5 and 7.0.

**Figure 2.** Turbidity change of the reacting solution during IPN microgel formation, as measured by UV/Vis spectrometer. Here 10 ml of aliquot solution was taken from the reaction container at the different reaction times and the PNIPAM concentration for each sample is  $1.27 \times 10^{-3}$  g/ml. The absorption wavelength is ranged from 290 nm to 500 nm.

**Figure 3.** The particle size distribution of the IPN microgel and its precursor PNIPAM microrgel at  $21^{\circ}\text{C}$ , as measured by dynamic light scattering. The scattering angle is at  $90^{\circ}$ .

**Figure 4.** Zimm plots of static light scattering for (a) PNIPAM microgel and (b) IPN micorgel at  $21^{\circ}\text{C}$ . The polymer concentration varies from  $2.5 \times 10^{-6}$  g/ml to  $1.0 \times 10^{-5}$  g/ml for both.

**Figure 5.** Temperature induced volume phase transition for PNIPAM and IPN microgels. They both exhibit the same volume phase transition temperature.

**Figure 6.** The viscosity change of the IPN semi-dilute aqueous solution with polymer concentration of  $2.5 \times 10^{-2}$  g/ml. Below  $\sim 34^{\circ}\text{C}$ , the dispersion is a fluid and above  $\sim 34^{\circ}\text{C}$ , the dispersion becomes a solid. The color of the dispersion is due to the Bragg diffraction from an ordered array of colloidal particles in water.

**Figure 7.** pH induced volume phase transition for PNIPAM and IPN microgels.

**Figure 8.** The particle size distributions of IPN micorgels at different pH environments.

**Figure 9.** The phase behavior of the PNIPAM-PAAc IPN nanoparticles in water.

- (a) The temperature-concentration phase diagram. There are six areas: (A) a homogeneous colloidal fluid, (B) a phase-separated colloidal fluid, (C) a colloidal crystal phase, (D) a colloidal glass, (E) a colloidal gel, and (F) a phase-separated colloidal gel.
- (b) Representative pictures of each phase: A) 1.0 wt%, 21 °C, B) 1.0 wt%, 36 °C, C) 2.5 wt%, 21 °C, D) 3.5 wt%, 21 °C, E) 4.5 wt%, 21 °C, and F) 4.5 wt%, 36 °C. The hydrodynamic radii of the PNIPAM and IPN particles at 20°C are 125 nm and 155 nm, respectively and used for Figures 9-10, where the weight ratio of PNIPA to PAAc within the IPN particles is 2:1, determined by both an evaporation method and static light scattering.

**Figure 10.** Temperature-dependent viscosity. Viscosities of aqueous solutions of IPN (C=1.97 w%), IPN (C= 3.27 w%) and PNIPAM (C=3.27 wt%) were measured as a function of temperature using a Brookfield Viscometer.

**Figure 11.** A cumulative release of model drugs from an *in situ*-formed gel depot. The dyes with molecular weights of 40, 70, 500 and 2000 k Daltons are mixed with 5.25 wt % IPN dispersion at room temperature, respectively. The weight ratio of PNIPAM to PAAc is 1:0.13 and the IPN particle size is 111 nm at room temperature. The release was measured after the IPN formed a gel in 37°C PBS.

#### Detailed Description of the Invention

The present invention comprises (1) The process, technique and apparatus for synthesizing of mono-disperse IPN nanoparticles with the interpenetrating structure of poly(N-isopropylacrylamide) and poly(acrylic acid) which includes (a) the reaction

kinetics of the IPN microgel formation, (b) laser light scattering study of IPN and PNIPA nanoparticles, (c) temperature induced volume phase transition and the thermo-thickening property and (d) pH induced volume phase transition. (2) A rich phase diagram exhibited by the semi-dilute IPN nanoparticle solutions opens a door for fundamental study of phase behavior of colloidal systems; (3) A thermally induced viscosity change, and *in situ* hydrogel formation for controlled drug release.

### **1. Reaction kinetics of the IPN microgel formation**

The kinetics of the IPN particle formation was studied by measuring the hydrodynamic radius ( $R_h$ ) of the particles as a function of reaction time as shown in Fig. 1. Here 10 ml of aliquot solution was taken from the reaction container at different reaction times, then purified via dialysis and finally diluted to  $5 \times 10^{-6}$  g/ml with distilled water for dynamic light scattering analysis. The solution concentration is based on the PNIPAM solid content. As one can see from Figure 1, initially, the PNIPAM microgels as seeds have an average hydrodynamic radius of 121 nm at 21°C. The value of  $R_h$  increases little during the first one hour, but dramatically in the following 60 minutes. Further reaction for 10 more minutes leads to precipitation. The data are well described by an equation of  $R_h = 119.1 + 1.77e^{t/\tau}$ , where the characterization time  $\tau = 31$  min. The particles grow faster as the reaction temperature increases.

Visual observation revealed that the solution turned from translucent to blurred blue to white and finally to precipitation during the IPN growth. This observation was quantified by measuring time dependent turbidity using an UV/Vis spectrometer as

shown in Fig. 2. Since the continuous reaction for 130 minutes lead to precipitation, the reaction was stopped at 120 min.

The IPN formation may be understood in terms of the polymerization of acrylic acid within each PNIPAM microgel. Although the PNIPAM microgels shrink slightly in acrylic acid solution due to an electrolyte effect, they swell enough at 21°C (below LCST) allowing the acrylic acid monomer to diffuse into their interior. The interaction between the –COOH group on acrylic acid and the –CONH- group on PNIPAM, in the form of monomeric or dimeric hydrogen bonding, [1] causes the preferred growth of the PAA network around the PNIPAM network. As the hydrophilic PAA concentration gradually increases in the PNIPAM skeleton, the IPN particle swells more by absorbing more water. Later reaction mainly happened on the IPN particle surface where there is much more un-reacted acrylic acid monomers available, resulting in fast growth of the particle size. The particles therefore underwent the structure change from PNIPAM to IPN and finally to IPN-PAAc core-shell throughout the reaction. The mechanism for the IPN synthesis is schematically shown in Scheme 1. To demonstrate the importance of hydrogen bonding for the IPN formation and growth, sodium acrylate was used to replace acrylic acid as an interpenetrating agent. Indeed, without hydrogen bonding PNIPAM-sodium acrylate cannot form an IPN structure as shown that there is no change in either turbidity or particle size within 4 hours, monitored by UV/Vis spectrometry and dynamic light scattering.

**2. Comparison of PNIPAM and IPN microgels at 21 °C** PNIPAM and IPN microgels were characterized and compared using dynamic and static light scattering. Both PNIPAM and IPN nanoparticles were diluted to  $5.0 \times 10^{-6}$  g/ml with distilled water

with pH values around 6.5-7.0. The particles size and distribution are shown in Fig. 3, in which the PNIPAM microgels are narrowly distributed with  $R_h$  around 121 nm, while IPN around 202 nm. The calculated polydispersity index (PD.I) for PNIPAM and IPN are 1.068 and 1.07, respectively. Here PD.I is defined as  $1 + \frac{\mu_2}{\langle \Gamma \rangle^2}$  with  $\mu_2 = \int_0^\infty G(D)(D - \langle D \rangle)^2 dD$  and  $D = \frac{K_b T}{6\pi\eta \langle R_h \rangle}$ . Increased particle size and their narrow distribution demonstrate that PAAc interpenetrates into the PNIPAM particles and the formation of new homo-PAAc particles during IPN synthesis is negligible.

Fig 4(a) shows the Zimm plot for the pure PNIPAM aqueous solution at 25°C, with sample concentration varying from  $2.5 \times 10^{-6}$  g/ml to  $1.0 \times 10^{-5}$  g/ml. The value of  $dn/dc$  used here is  $0.166 \text{ cm}^3/\text{g}$ , measured by a refractometer. From the extrapolation of  $KC/R_{vv}(q)$  in Eq.1 to the zero angle and zero concentration, the molar mass  $M_w$ , the second virial coefficient  $A_2$ , and the radius of gyration  $\langle R_g \rangle$  are determined to be  $8.14 \times 10^7 \text{ g/mol}$ ,  $8.90 \times 10^{-5} \text{ mol} \cdot \text{cm}^3/\text{g}^2$ , and 98 nm, respectively. By combining DLS and SLS results, the ratio of  $\langle R_g \rangle / \langle R_h \rangle$  was found to be 0.80, which is close to the theoretical value of  $(3/5)^{1/2}$  for a uniform hard sphere. The density of a pure PNIPAM nanoparticle ( $\rho$ ) in water is estimated about  $1.82 \times 10^{-2} \text{ g/cm}^3$  at 25°C in water using the equation  $4/3 * \pi R_h^3 \rho = M_w / N_A$ , where  $R_h$  and  $M_w$  are obtained from DLS and SLS, respectively, and  $N_A$  is Avogadro's number.

From the Zimm plot of static light scattering for IPN microgels in water as shown in Fig 4(b), the molar mass  $M_w$ , the radius of gyration  $\langle R_g \rangle$  and second virial coefficient  $A_2$  are  $2.34 \times 10^8 \text{ g/mol}$ , 144 nm and  $9.50 \times 10^{-5} \text{ cm}^3/\text{g}^2$ , respectively. The value of  $dn/dc$  used here is  $0.102 \text{ cm}^3/\text{g}$ . The increased value of  $A_2$  for the IPN indicates that the IPN is

more hydrophilic than its PNIPAM precursor at a neutral pH environment. As a result, the IPN contains more water than the PNIPAM does. Combining DLS and SLS results, we obtain the ratio of  $\langle R_g \rangle / \langle R_h \rangle$  to be 0.71. It suggests that the polymers are uniformly distributed. The average density of this IPN ( $\rho$ ) is estimated about  $1.13 \times 10^{-2}$  g/cm<sup>3</sup> at 25°C in water. The detailed comparison between PNIPAM and IPN microgels is listed in Table 1.

The weight ratio of PAAc to PNIPAM in each IPN microgel is determined to be 1.88:1 by calculating the molar weight ratio of the IPN ( $M_w 2.34 \times 10^8$  g/mol) to the PNIPAM ( $8.14 \times 10^7$  g/mol). The value is very close to 1.82:1, measured by the evaporation method. If the reaction lasted longer, the weight ratio increased correspondingly.

### **3. Temperature induced volume phase transition and the thermo-thickening property**

The IPN microgel undergoes the volume phase transition at 34 °C that is the same as the one for the PNIPAM microgel as shown in Fig. 5. For a randomly co-polymerized PAAc/PNIPAM gel, the volume phase transition temperature increases with PAAc concentration.[8] The volume change of the IPN below and above the volume transition temperature is smaller than that of the PNIPAM. This is because the PAAc network in the IPN is not sensitive to the temperature change and can reduce the shrinkage of the PNIPAM network.

For diluted IPN and PNIPAM solution ( $5.0 \times 10^{-6}$  g/ml), the interaction between particles can be neglected. However, as polymer concentration increases, the interaction between particles plays an important role that causes viscosity to change as the

temperature changes. Specifically, a semi-diluted IPN aqueous solution with polymer concentration 2.5% g/ml is found to exhibit an inverse thermoreversible gelation at pH above 5. That is, when the system is heated to above the gelation temperature  $T_g=34^{\circ}\text{C}$ , it undergoes a transformation from a low-viscous fluid to a gel. This behavior is completely reversible. Fig. 6 shows the comparison of IPN semi-diluted solution at room temperature (left) and  $40^{\circ}\text{C}$  (right). The PNIPAM in the IPN matrix provides physical crosslinking bonds between particles via a temperature-dependent interparticle potential, [22] while PAA in the IPN in the neutral pH provides ionic charges that are temperature-independent and prevent the collapse of the particles into an aggregate. In contrast to polymer solutions that have the inverse thermoreversible gelation such as methyl cellulose,[16] poly(ethylene oxide)-poly(propylene oxide)-poly(ethylene oxide) triblock copolymers,[17] PNIPAM-PAA copolymers,[18] and degradable triblock copolymers,[19] the particles in our system can self-assemble into an ordered structures, displaying colors due to the Bragg diffraction.[23]

**4. pH induced volume phase transition** The IPN microgel possesses a pH sensitivity due to the contribution of the PAAc. The values of  $R_h$  for IPN and PNIPAM microgels with the polymer concentration of  $5.0 \times 10^{-6}$  g/ml at  $21^{\circ}\text{C}$  are shown in Fig. 7 as a function of pH. The pH values were adjusted by adding either hydrochloric acid or sodium hydroxide to the solution. As shown in Fig. 7, there is a sharp drop of  $R_h$  for the IPN microgel from 200 nm to 165 nm as the pH decreases from 5 to 4. In the pH range of 5-10, the  $R_h$  is around 200 nm without aggregation as demonstrated by a constant scattering light intensity. It is well known that PAAc is in an ionic state when the pH is above its pKa 4.7 and is hydrophilic. However, at  $\text{pH} < 4.7$ , the PAAc is the molecular

state and becomes hydrophobic, repelling water out from its network. This causes the shrinkage of the IPN at low pH value. It's interesting to note that the extent of pH induced the IPN shrinkage is about the same as that of the temperature induced the IPN shrinkage, both from 200 nm to around 160 nm. As expected, there is no particle size variation observed for the PNIPAM microgel in the pH range of 4-10. The slight decrease occurred at pH=2 may be due to the electrolyte effect. The comparison of the IPN microgel size distributions at pH 4 and 7 is shown in Figure 8. The PD. I for IPN microgel at pH 4 and 7 are 1.02 and 1.07, respectively. It indicates that the IPN has a narrower size distribution after the shrinkage at pH 4.

**5. Phase diagram of the semi-dilute IPN nanoparticle aqueous solution** The aqueous solutions of the IPN nanoparticles exhibit rich phase behavior as shown in Figure 9 (a), determined by combining visual inspection, turbidity and viscosity measurements. The phase behavior has been divided into six areas with typical optical appearances as shown in Figure 9 (b). At low polymer concentrations ( $< 2.2 \times 10^{-2}$  g/ml, Area A), the IPN dispersions appear translucent and flow easily. The IPN nanoparticles are fully swollen. Upon increasing the temperature, the particle size shrinks and the dispersions enter into a phase-separated area (Area B). In the intermediate polymer concentration range (between  $2.2$  and  $3.0 \times 10^{-2}$  g/ml, Area C), the IPN dispersions are colloidal crystal fluids at room temperature. These crystals are easy to observe due to their iridescent patterns caused by Bragg diffraction.<sup>[24]</sup> Iridescent color resulting from the Bragg diffraction of visible light by the periodic structure of bilayer membranes has been also reported before.<sup>[25]</sup> Constructive interference occurs if the Bragg condition,  $2nd\sin\theta = m\lambda$ , is satisfied, where  $d$ ,  $\theta$ ,  $n$ ,  $\lambda$ , and  $m$  are the lattice spacing, the diffraction

angle, the refractive index of the gel medium, the wavelength of light in vacuum and an integer, respectively. In a high polymer concentration range (between  $3.0 \times 10^{-2}$  and  $4.0 \times 10^{-2}$  g/ml, Area D), the IPN dispersions are colloidal glass fluids that are viscous fluids and exhibit a homogeneous color due to a short-range order.<sup>[23]</sup> At very high polymer concentrations ( $>4 \times 10^{-2}$  g/ml, area D) at room temperature, the IPN dispersions become colloidal gels. At higher temperatures, the gels become white and opaque (Area F).

The inverse thermoreversible gelation occurs in a broad polymer concentration above  $2.5 \times 10^{-2}$  g/ml. That is, when the system is heated to above the gelation temperature  $T_g$ , it undergoes a transformation from a low-viscous fluid to a gel. This behavior is completely reversible. A typical temperature-dependent viscosity of an IPN nanoparticle aqueous solution (3.27 wt %) is presented in Figure 10 in comparison with that for a PNIPAM nanoparticle dispersion with the same polymer concentration with a heating rate of  $2\text{C}^{\circ}/5\text{mins}$ . The viscosity was measured using a Brookfield viscometer with a shear rate of 100 rpm. The viscosity data obtained with various heating rates between 1 and  $5\text{ C}^{\circ}/5\text{mins}$  were the same, indicating that the associative phenomenon is rather fast.

The viscosity of the PNIPAM nanoparticle dispersion ( $C=3.27$  wt %) was observed to decrease as the temperature increased and reached a plateau above  $32^{\circ}\text{C}$ . This was due to the increase of the mobility of individual particles and the gradually shrinking particle size with the increasing temperature. In comparison, the IPN nanoparticle dispersion ( $C=3.27$  wt %) exhibited behavior similar to the PNIPAM dispersion below  $32^{\circ}\text{C}$ . However, when the temperature reached  $32.5^{\circ}\text{C}$ , the viscosity

drastically increased and jumped beyond our viscometer's measurement range. Visual inspection revealed that the dispersion in the test tube was physically gelled and could not flow even the tube was set upside down. The thermally-induced viscosity change can be tuned by changing polymer concentration. The IPN dispersion with a lower polymer concentration ( $C < 2.5 \times 10^{-2}$  g/ml) exhibits a viscosity enhancement but without gelling, as shown in Figure 10. The gelation of the IPN dispersion at  $T > T_g$  may be caused by the attractive interactions between particles. At room temperature, PNIPAM particles are in the swollen state and they contain 97% water by volume. The van der Waals attraction between colloidal particles is negligible due to the close match in the Hamaker constants of the particle and the water.<sup>[26]</sup> The reduced osmotic second virial coefficient exhibits a sharp change at the volume transition temperature, beyond which it turns negative. Thermodynamic calculation indicates that the reduced interaction potential energy between nanoparticles increases by over six orders of magnitude as temperature changes from 24°C to 36 °C, with the sharpest increase near the volume transition temperature of 34 °C.<sup>[26]</sup> The gelation may be achieved by the balance between van der Waal interaction between PNIPAM networks and the ionic repulsion of the PAAc networks in the IPN particles. It is noted that the temperature-dependent interparticle potential is also responsible to the formation of reversible or irreversible aggregates in colloidal systems of PNIPAM derivatives.<sup>[10]</sup> More convincing evidences are needed to determine the exact origin of the attractive force that bonds the IPN nanoparticles into a network at  $T > T_g$ .

**6. Controlled drug delivery from the *in situ* physically crosslinked IPN nanonanoparticle networks.** One of the key applications of this novel hydrogel nanoparticle dispersion is in the area of controlled drug delivery. The mixture of the IPN

nanoparticles and drugs can be prepared as an aqueous solution below the gelation temperature to form a drug delivery liquid. This liquid could be administrated into a warm-blooded animal which forms *in situ* a gelled drug depot since body temperature will be above the gelation temperature of the IPN dispersion. The drug can be entrapped inside a hydrogel by solution mixing without chemical reaction. In contrast to hydrogels obtained from polymer solutions with inverse thermoreversible gelation,<sup>[19]</sup> the hydrogel formed with our nanoparticle dispersions has unique two-level structural hierarchy: the primary network consists of crosslinked polymer chains inside each nanoparticle, while the secondary network is a crosslinked system of the nanoparticles. The drug could be entrapped either between the particles or inside each particle.

As a demonstration, we used dextran with different molecular weights as a model drug and mixed them with an IPN nanoparticle dispersion with a polymer concentration at 5.25 wt%. At room temperature, the dispersion is a viscous fluid can be mixed with a dextran solution very thoroughly. The drug-dispersion mixture was then heated to 37 °C at which point the dispersion becomes a gel. This gel was then taken out from the tube and immersed into a PBS solution at 37 °C. The cumulative drug release from the gel was measured using a UV-Visible spectrophotometer as a function of time as shown in Figure 11. It is clear that the molecules with smaller molecular weights diffuse out faster than those of higher molecular weights. The release rates slowed down gradually for 70K, 500K and 2M drug analogs in the order of their molecular weights. The drug molecules here were entrapped between IPN nanoparticles, permitting the release of molecules with very large molecular weight of 2M. It is worth further investigation to increase the difference of the release rates for dextrans with different molecular weights

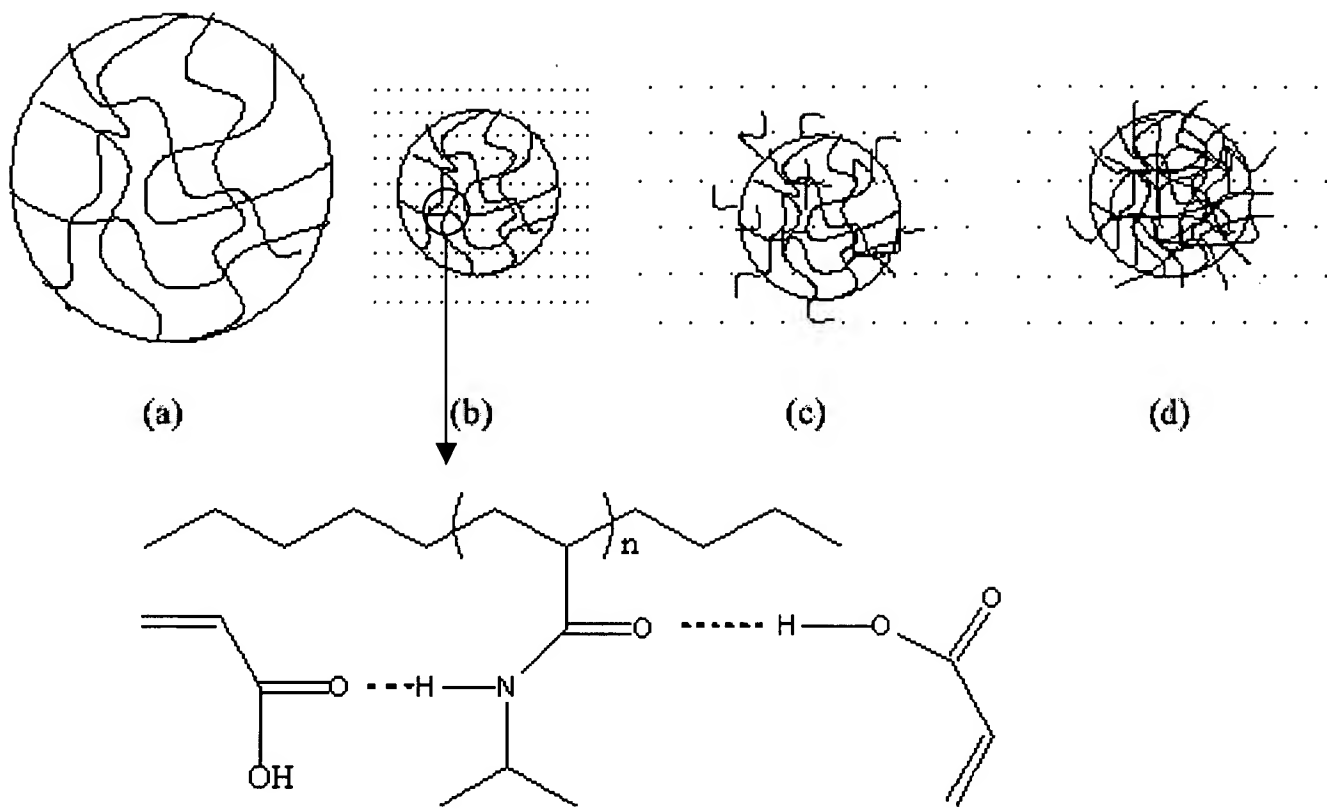
by optimizing synthesis conditions. It is noted that the polymer concentration used in the release experiment is about 10 times smaller than that used in a polymer solution system.

[18]

## **CLAIMS**

We Claim:

1. The process, technique and apparatus for synthesizing of mono-disperse IPN nanoparticles with the interpenetrating structure of poly(N-isopropylacrylamide) and poly(acrylic acid) which includes a) The reaction kinetics of the IPN microgel formation, b) laser light scattering study of IPN and PNIPA nanoparticles, c) Temperature induced volume phase transition and the thermo-thickening property and d) pH induced volume phase transition.
2. A rich phase diagram exhibited by the semi-dilute IPN nanoparticle solutions opens a door for fundamental study of phase behavior of colloidal systems.
3. A thermally induced viscosity change, and *in situ* hydrogel formation for controlled drug release.



Scheme 1

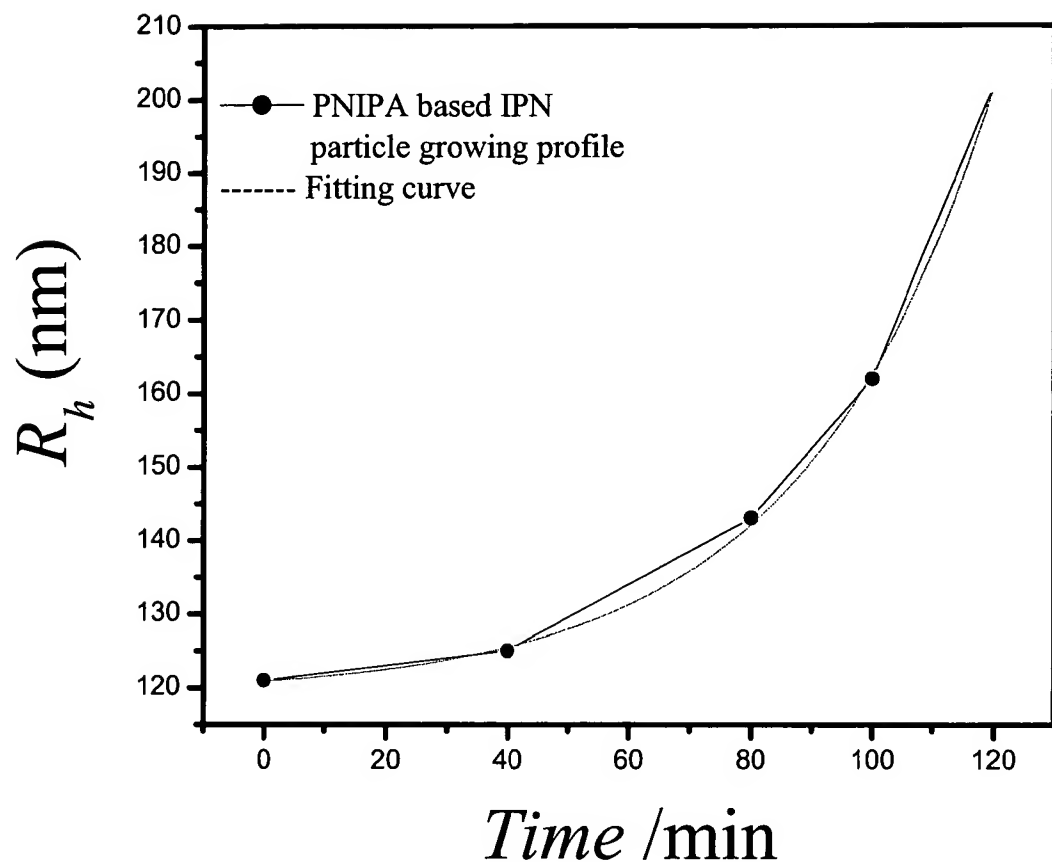


Figure 1.

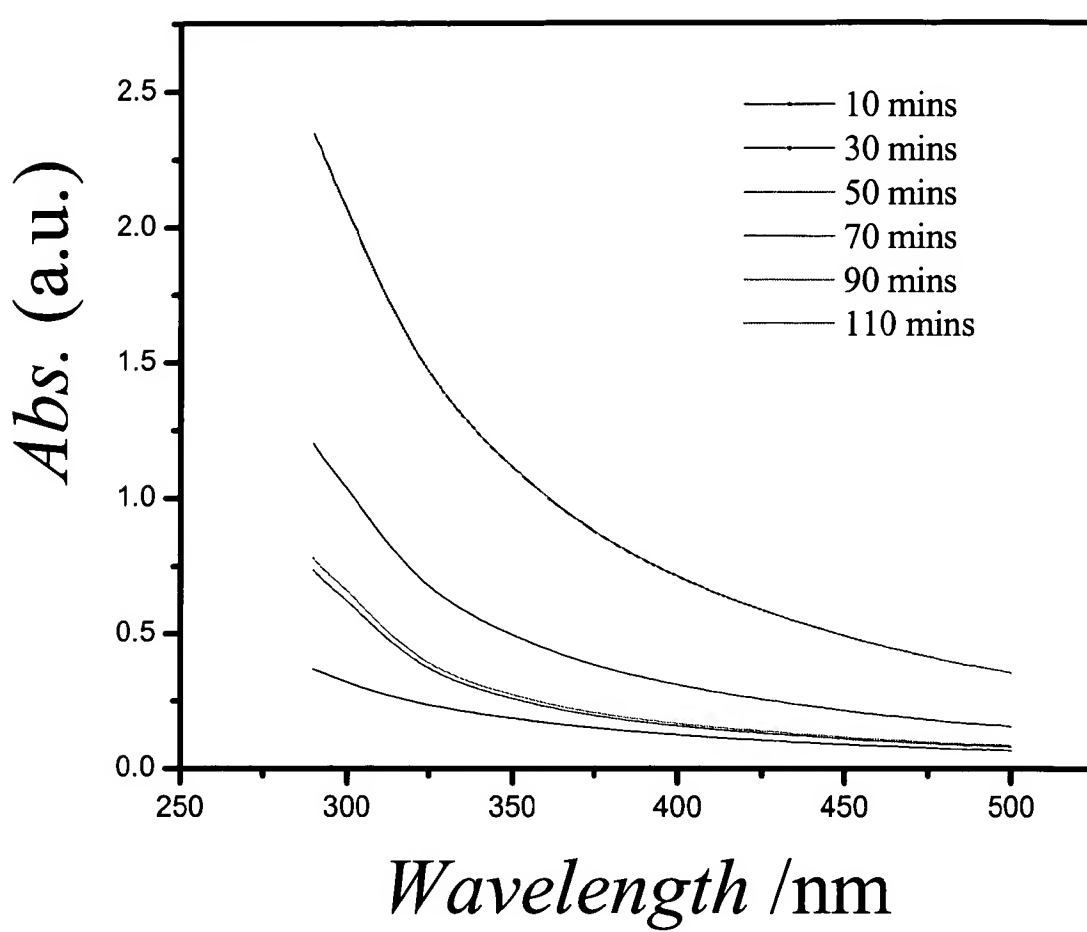


Figure 2

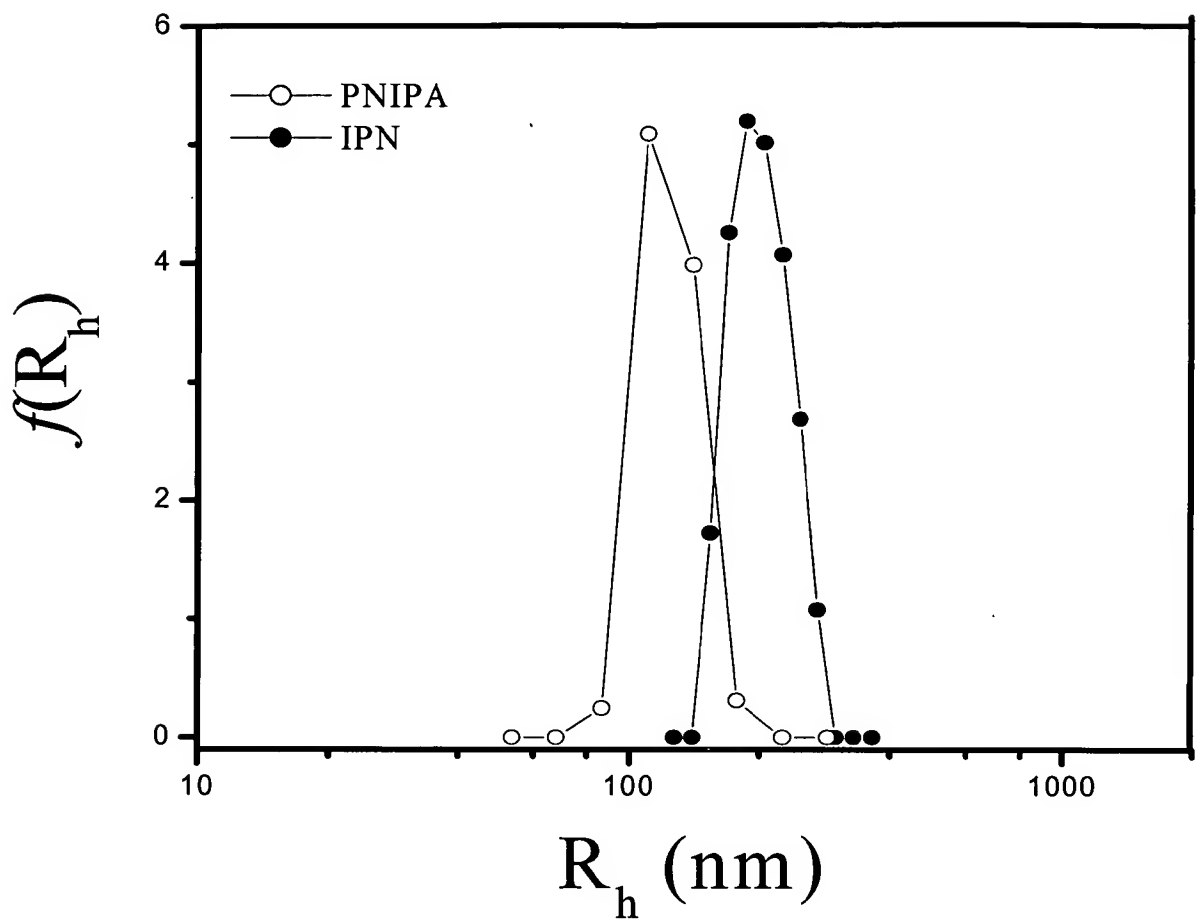


Figure 3

BEST AVAILABLE COPY

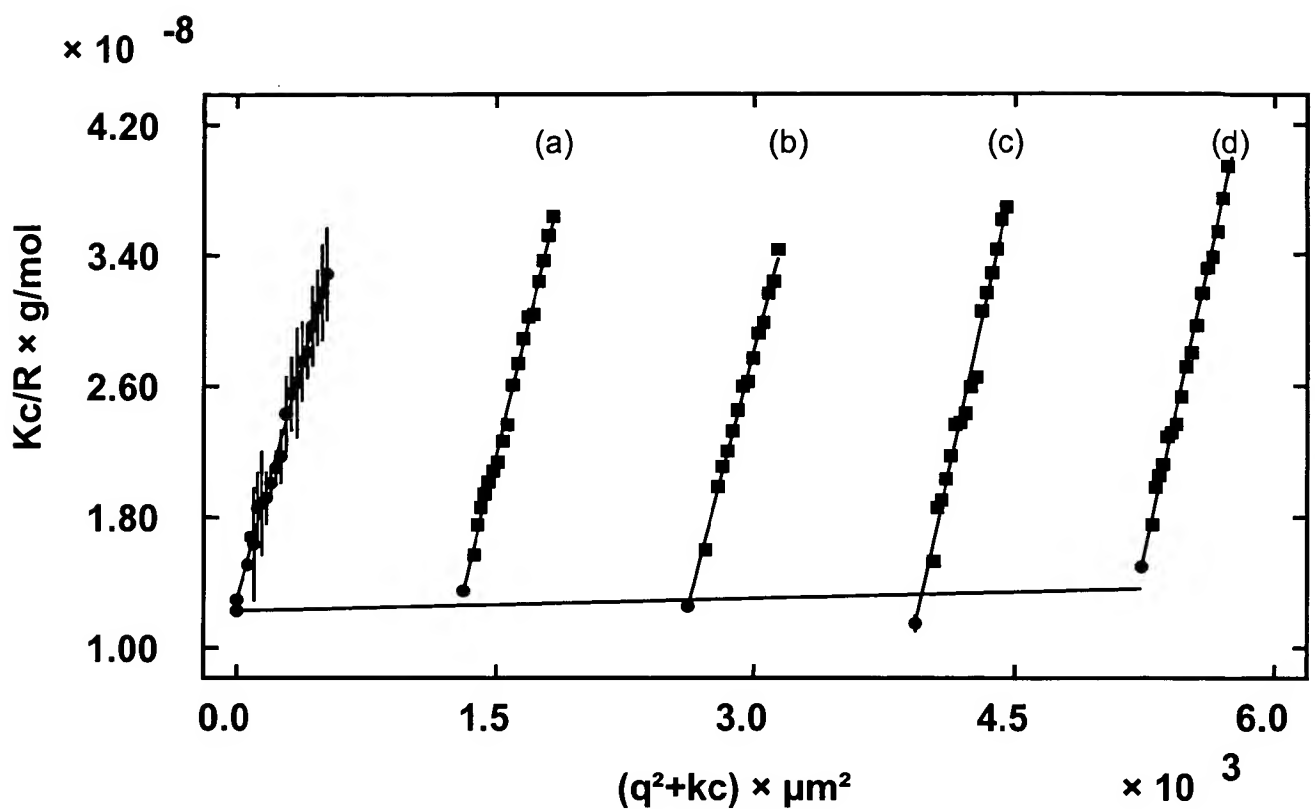


Figure 4(a)

BEST AVAILABLE COPY

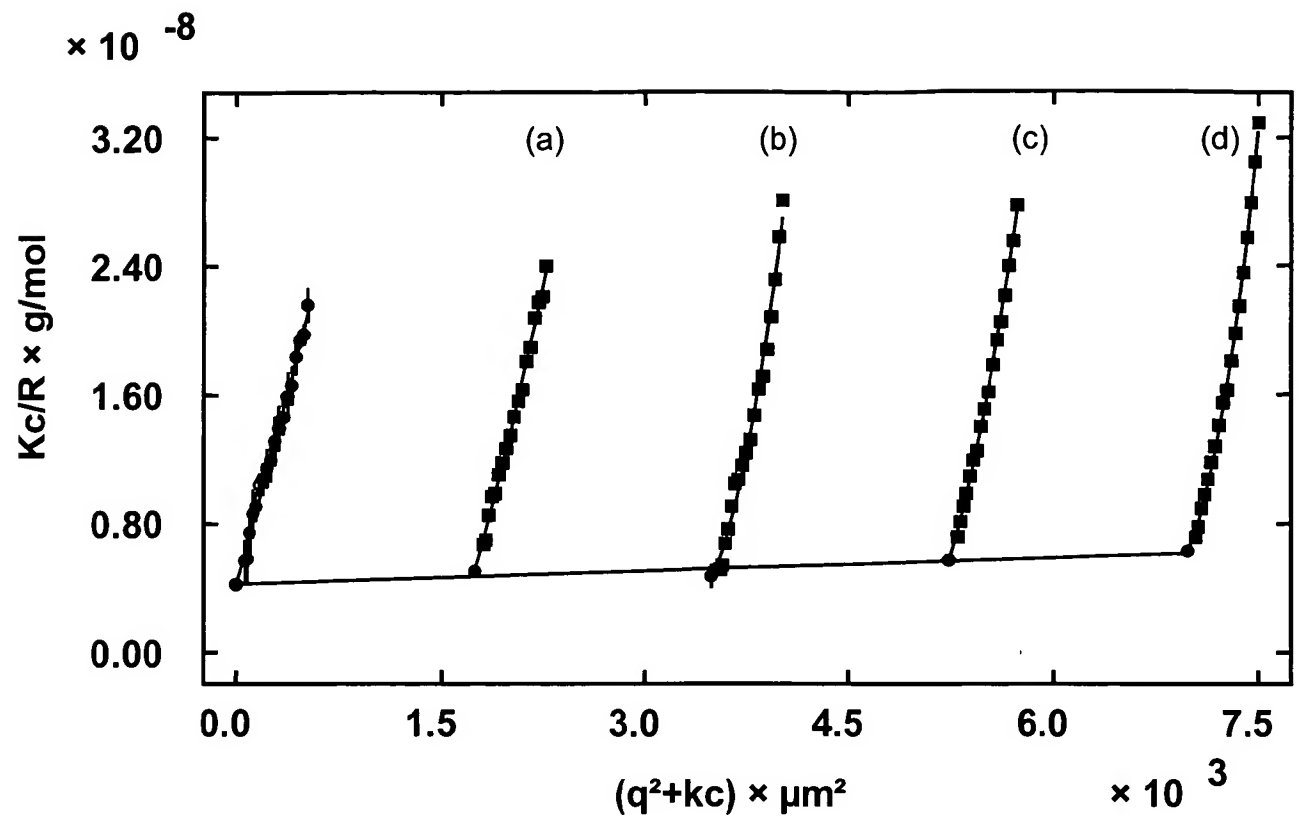


Figure 4(b)

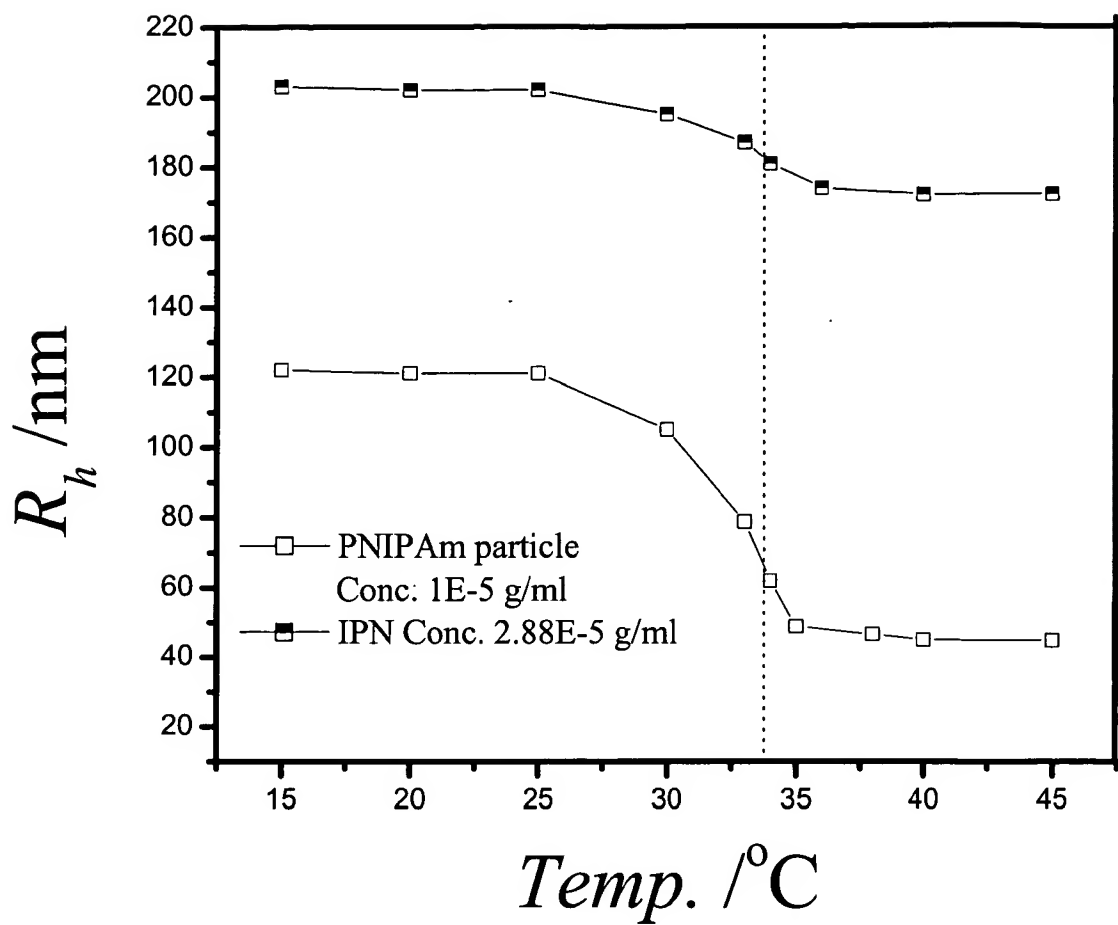


Figure 5.

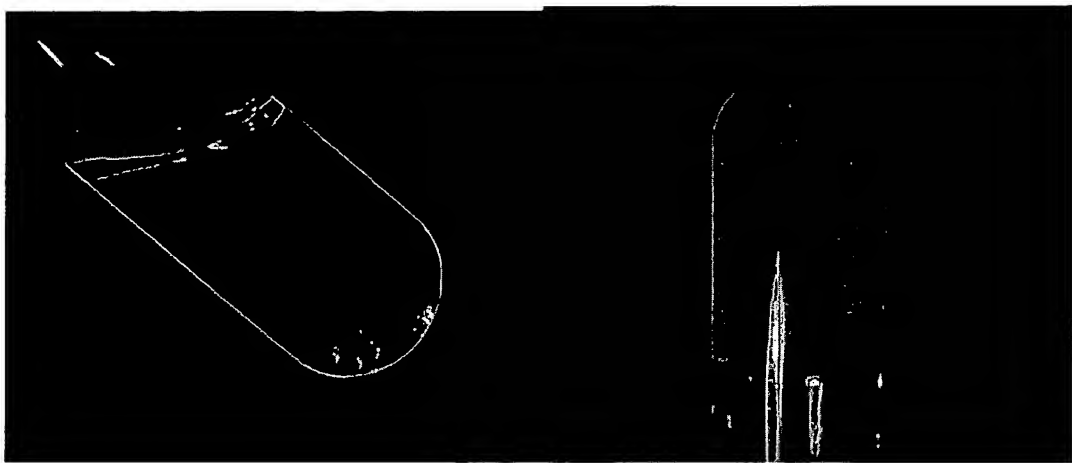


Figure 6

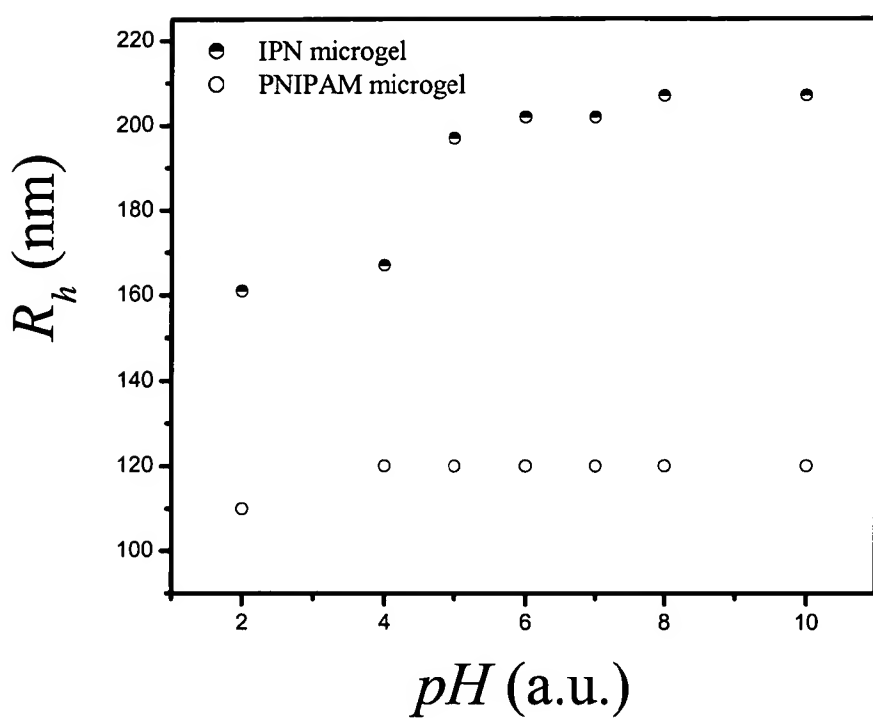


Figure 7.

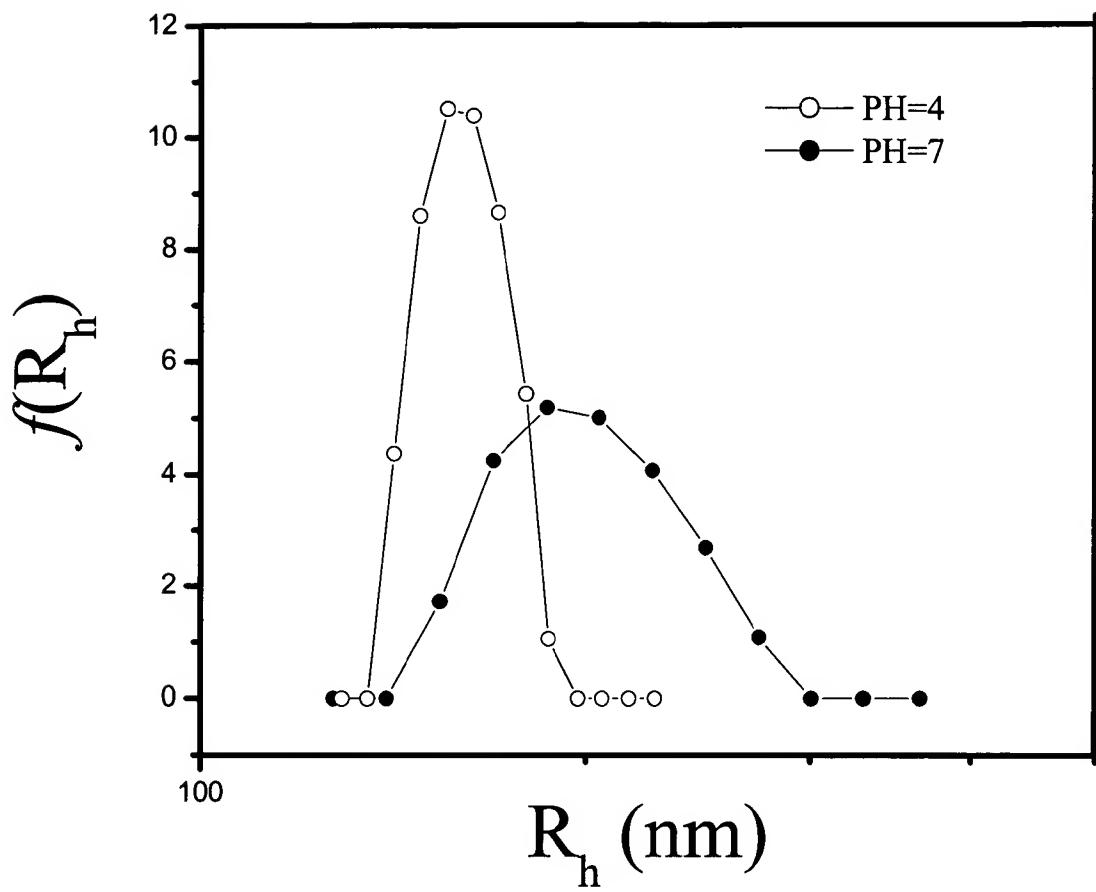


Figure 8.

**Table 1. Comparison of PNIPA and IPN Nanoparticles**

	R <sub>h</sub> (nm)	R <sub>g</sub> (nm)	R <sub>g</sub> /R <sub>h</sub> (a.u.)	A <sub>2</sub> (mol*cm <sup>3</sup> /g <sup>2</sup> )	Mw (g/mol)	Density(g/cm <sup>3</sup> )	PNIPA:PAA ratio
PNIPA	121	98	0.81	8.9x10 <sup>-5</sup>	8.137x10 <sup>7</sup>	1.82x10 <sup>-2</sup>	1 : Nothing
IPN	202	143	0.71	9.5x10 <sup>-5</sup>	2.341x10 <sup>8</sup>	1.13x10 <sup>-2</sup>	1 : 1.88

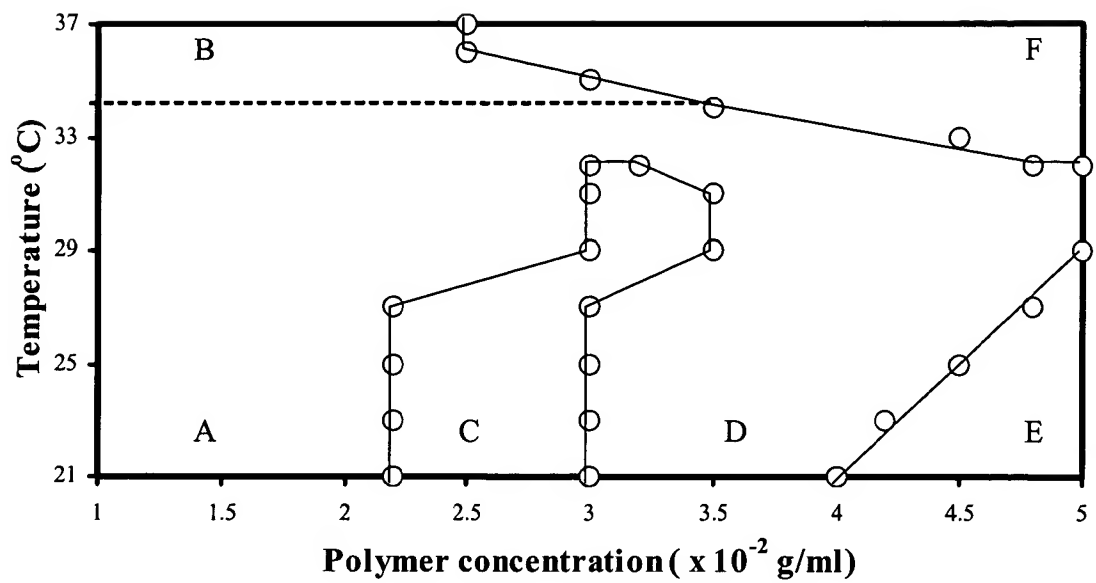


Figure 9(a).

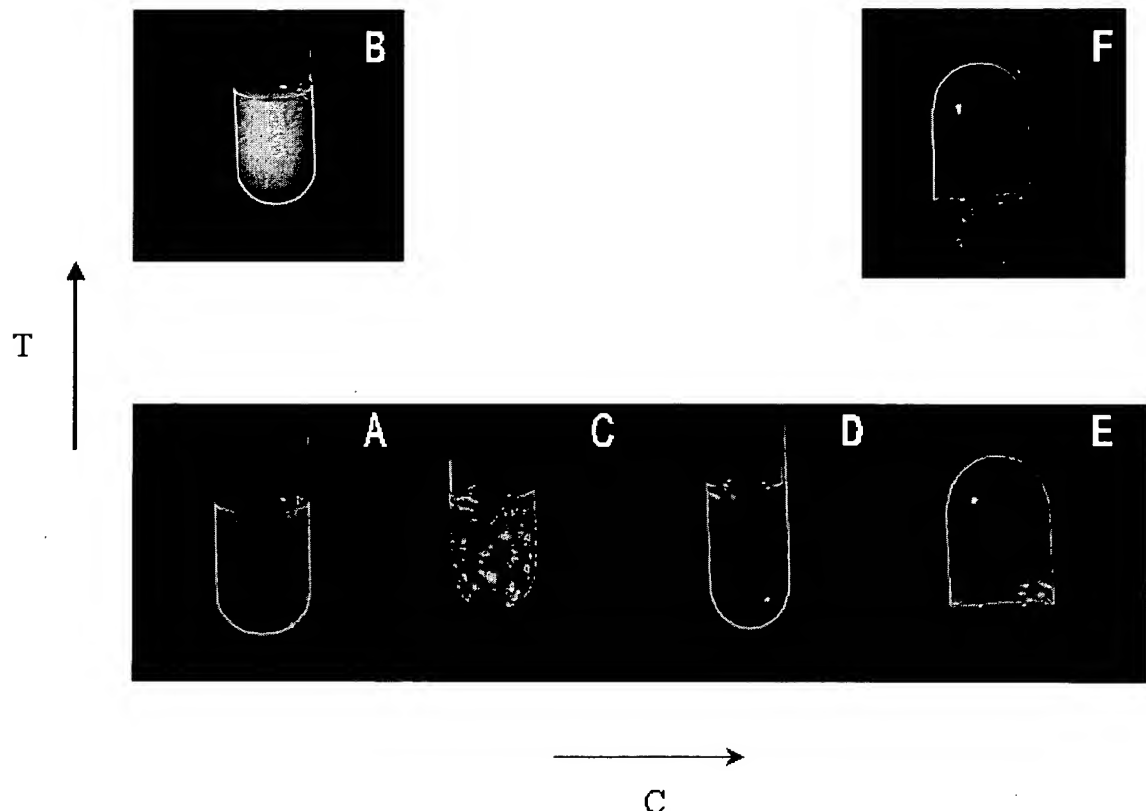
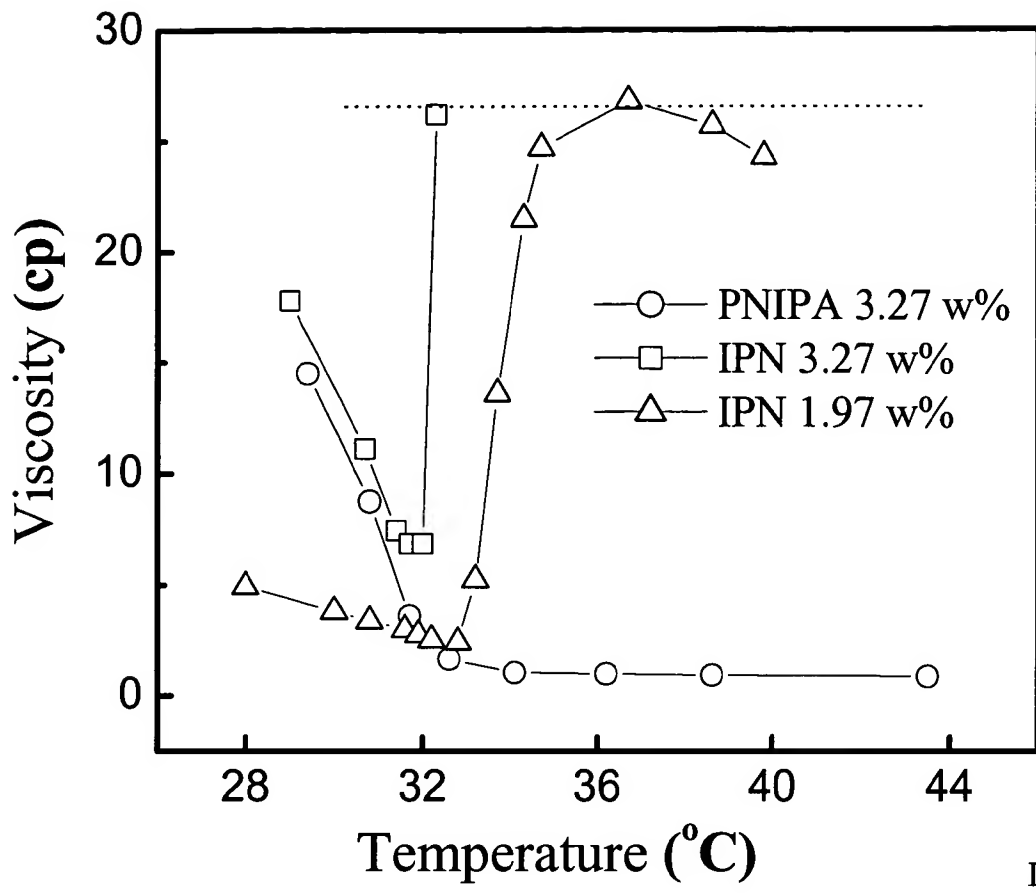


Figure 9(b).



Dr. Z. Hu

Figure 10.

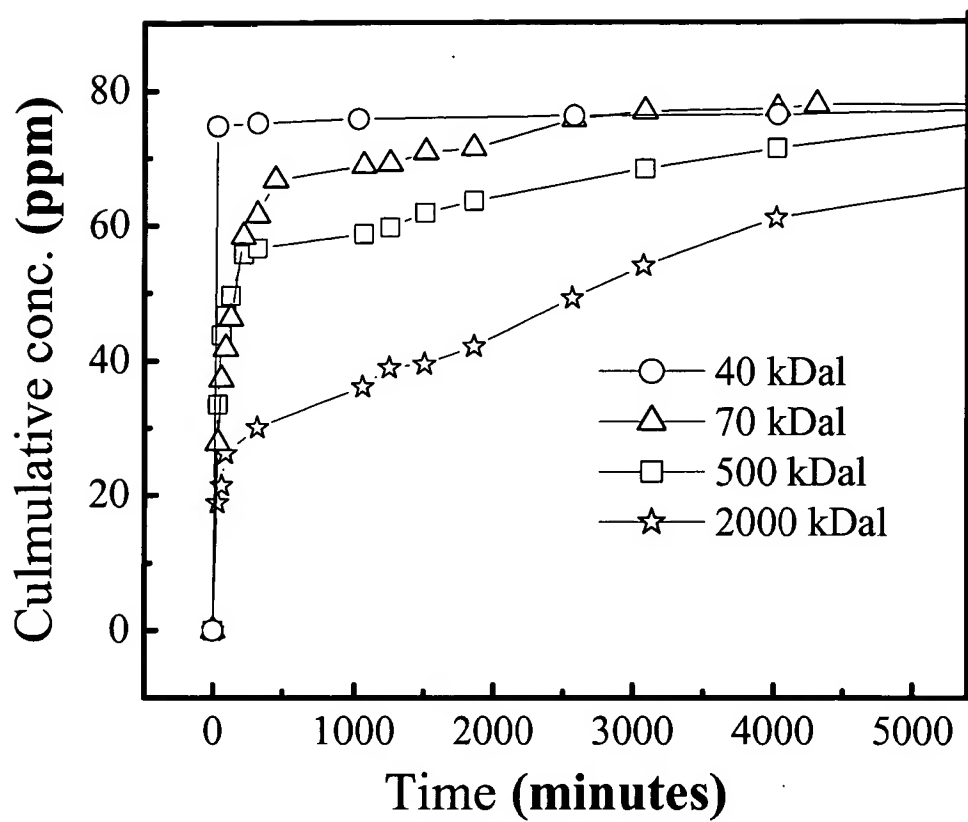


Figure 11.